Applications of SPH with the acceleration correction algorithm in structural impact computations

Amit Shaw and S. R. Reid*

School of Engineering, University of Aberdeen, Aberdeen AB24 3UE, United Kingdom

How to use artificial viscosity 'properly' (i.e. without excessively effecting the physics of the response) in smooth particle hydrodynamics (SPH) computations has been a long standing issue. Though SPH has great potential in problems related to dynamic structural mechanics, the loss of kinetic energy due to the 'inaccurate' choice of artificial viscosity parameters may result in physically unreal phenomena. Recently, the effect of artificial viscosity in SPH computations has been revisited and an acceleration correction algorithm to recover the majority of the 'lost' kinetic energy has been proposed by Shaw and Reid (2009). The essence of the acceleration correction algorithm is to calculate the change in the acceleration due to the artificial viscosity term and then correct the computed acceleration by subtracting a convex approximation of the 'changed' acceleration. The energy equation is accordingly modified. In the process, some of the unwanted energy dissipation is removed while retaining the basic effect of the artificial viscosity in order to have a stable computation. The approach used is relatively straightforward and, in due course, this approach will be optimized.

In this article, some additional numerical aspects of the acceleration correction algorithm are discussed and the method is further explored in the context of some classical elastic-plastic impact problems. It is shown that, together with the acceleration correction algorithm, SPH can be used as a useful tool in dynamic, inelastic structural mechanics.

Keywords: Acceleration correction algorithm, artificial viscosity, energy dissipation, smooth particle hydrodynamics.

Introduction

WHILE the application of the smooth particle hydrodynamics (SPH) in astrophysical problems has a long history[1–3], its application to dynamic structural mechanics, in particular to elasto-plastic problems related to impact mechanics is relatively new. SPH was first extended to problems in solid mechanics by Libersky and Pteschek[4] and Libersky *et al.*[5]. Thereafter several attempts have been made to apply SPH for the numerical modelling of high velocity impact and penetration problems[6,7]. Due to its particle nature, SPH is very effective in modelling fragmentation and material separation which may be caused by the formation of cracks and crack systems, formed by the coalescence of a multitude of small crack-like flaws[8], physical phenomena encountered in several areas of impact mechanics, which are not easily dealt with by other methods. However the method is not yet in general use as a standard tool in dynamic structural mechanics due to some inherent computational difficulties. These include the use of the artificial viscosity to promote numerical stability, perhaps one of the major stumbling blocks. While artificial viscosity is useful in order to model the effects of shock waves and other phenomena caused by the discontinuous initial condition of physical quantities (velocity, pressure, etc.), its improper use may introduce excess dissipation which results in increasing the entropy of the system and physically unreal behaviour.

In an artificial viscosity formulation, whenever the system, say a gas, experiences any shock compression (local jumps in physical quantities), an artificial viscous term is introduced in the momentum equation as

$$\frac{\mathrm{d}v}{\mathrm{d}t} = -\frac{1}{\rho}\nabla(p+\Pi), \quad (1)$$

where v, ρ and p are respectively the velocity, density and pressure in the shock compression zone. There are many forms of the artificial viscosity parameter Π present in the literature. Nevertheless they have a common generic form

$$\Pi = \alpha_1 \rho c_s |\Delta \boldsymbol{v}| + \alpha_2 \rho |\Delta \boldsymbol{v}|^2, \quad (2)$$

where $\Delta \boldsymbol{v}$ is the velocity difference across the shock compression zone and (α_1, α_2) are the parameters which define the strength of the artificial viscosity. The most basic, physical property that artificial viscosity generates is energy dissipation, i.e. it converts kinetic energy into

*For correspondence. (e-mail: steve.reid@abdn.ac.uk)

internal energy. However one has to be careful, when choosing the artificial viscosity parameters (α_1, α_2), that it does not induce the equivalent of a 'false' pressure which may lead to excessive loss of kinetic energy and make the system over-dissipative, the predictions becoming correspondingly unreal. This is of particular concern in impact mechanics problems. Unfortunately there is not any standard set of parameters which work for a wide range of problems. The 'ideal' situation would be when the form of artificial viscosity does not need any user-specified parameters and yet stabilizes the numerical computation, without adding unwanted dissipation into the system.

In order to accomplish the above mentioned objective, Shaw and Reid[9] recently proposed an acceleration correction algorithm. The essence of the method is to calculate the change in the acceleration due to the artificial viscosity term and then correct the computed acceleration by subtracting a convex approximation of the 'changed' acceleration. The energy equation is also modified accordingly. It is shown in Shaw and Reid[9], exemplified by three elastic and elastic-plastic impact problems, that the acceleration correction algorithm is capable of removing the majority of the unwanted dissipation while retaining the basic numerical effect of the artificial viscosity to produce a stable computation.

Some additional numerical aspects of the acceleration correction algorithm are discussed here and the method is further explored in the context of a classical elastic-plastic impact problem. The superior performance of the acceleration correction algorithm vis-à-vis the SPH procedures with standard artificial viscosity is discussed.

SPH – a brief overview

Governing equations

The conservation equations for continuum mechanics are

$$\frac{\mathrm{d}\rho}{\mathrm{d}t} = -\rho\frac{\partial v^{\alpha}}{\partial x^{\beta}}, \tag{3}$$

$$\frac{\mathrm{d}v^{\alpha}}{\mathrm{d}t} = -\frac{1}{\rho}\frac{\partial \sigma^{\alpha\beta}}{\partial x^{\beta}}, \tag{4}$$

$$\frac{\mathrm{d}e}{\mathrm{d}t} = -\frac{\sigma^{\alpha\beta}}{\rho}\frac{\partial v^{\alpha}}{\partial x^{\beta}} \tag{5}$$

and

$$\frac{\mathrm{d}x^{\alpha}}{\mathrm{d}t} = v^{\alpha}, \tag{6}$$

where for any material point, ρ denotes its mass density, e the specific internal energy, v^{α} and $\sigma^{\alpha\beta}$ are respectively the element of velocity and Cauchy stress tensor, x^{α} the spatial coordinate, d/dt the time derivative taken in the moving Lagrangian frame and the superscript 'α' indicates the spatial direction. In eqs (3)–(6), the effect of heat conduction is neglected assuming that the deformation process is locally adiabatic. The stress component in eqs (4) and (5) may be written in terms of hydrostatic and deviatoric stresses as

$$\sigma^{\alpha\beta} = P\delta^{\alpha\beta} - S^{\alpha\beta}, \tag{7}$$

where P and $S^{\alpha\beta}$ are respectively the pressure and the components of the traceless symmetric deviatoric stress tensor. The pressure in eq. (7) may be calculated through an equation of state, which is generally a function of density (ρ) and the specific internal energy (e). The most commonly used equation of states for elastic-plastic problems is the Mie–Gruneisen equation given by

$$P(\rho,e) = \left(1-\frac{1}{2}\Gamma\eta\right)P_H + \Gamma\rho e, \tag{8}$$

where

$$P_H = a_0\eta + b_0\eta^2 + c_0\eta^3 \text{ for } \eta > 0 \text{ and } P_H = c_0\eta^3 \text{ for } \eta < 0, \tag{9}$$

$$\eta = \left(\frac{\rho}{\rho_0} - 1\right), \tag{10}$$

$$a_0 = \rho_0 C^2, \tag{11}$$

$$b_0 = a_0[1 + 2(S-1)], \tag{12}$$

$$c_0 = a_0[2(S-1) + 3(S-1)^2]. \tag{13}$$

Here, S and C are parameters describing the linear shock-velocity and particle-velocity relation and Γ is the Gruneisen parameter.

Now, the Jaumann stress rate is given by

$$\dot{S}^{\alpha\beta} = \mu\left(\dot{\varepsilon}^{\alpha\beta} - \frac{1}{3}\delta^{\alpha\beta}\dot{\varepsilon}^{\gamma\gamma}\right) + S^{\alpha\gamma}\dot{R}^{\beta\gamma} + S^{\gamma\beta}\dot{R}^{\alpha\gamma}, \tag{14}$$

where μ is the shear modulus. The component $\dot{\varepsilon}^{\alpha\beta}$ of the strain rate tensor and $\dot{R}^{\alpha\beta}$ of the spin tensor may be obtained as

$$\dot{\varepsilon}^{\alpha\beta} = \frac{1}{2}\left(\frac{\partial v^{\alpha}}{\partial x^{\beta}} + \frac{\partial v^{\beta}}{\partial x^{\alpha}}\right), \tag{15}$$

$$\dot{R}^{\alpha\beta} = \frac{1}{2}\left(\frac{\partial v^{\alpha}}{\partial x^{\beta}} - \frac{\partial v^{\beta}}{\partial x^{\alpha}}\right). \tag{16}$$

The plastic flow régime is determined by the Von Mises yield criterion given as

$$\sigma_e - \sigma_y \le 0, \tag{17}$$

where

$$\sigma_e = \sqrt{3S^{\alpha\beta}S^{\alpha\beta}}$$

is the Von Mises effective stress and σ_y is the yield stress. At every time step the effective stress σ_e is checked and if it exceeds the yield stress σ_y, the individual stress components are brought back to the yield surface as explained by Shaw and Reid[9] using

$$S^{\alpha\beta} = fS^{\alpha\beta}, \text{ where } f = \min\left\{\frac{\sigma_y}{\sqrt{3}J_2}, 1\right\}.$$

Discretization of governing equations

In smooth particle hydrodynamics, first the computational domain is discretized by a set of particles. Each particle, say the ith particle, is associated with mass m_i, density ρ_i, velocity component v_i^α, internal energy e_i, elastic wave speed c_i, pressure P_i, deviatoric stress component $S_i^{\alpha\beta}$ and the Cauchy stress component $\sigma_i^{\alpha\beta} = P_i - S_i^{\alpha\beta}$. Then the semi-discrete form of the governing equations is obtained through a kernel approximation as[4,5]

$$\frac{\mathrm{d}\rho_i}{\mathrm{d}t} = \rho_i \sum_j \frac{m_j}{\rho_j}(v_i^\beta - v_j^\beta)W_{ij,\beta}, \tag{18}$$

$$\frac{\mathrm{d}v_i^\alpha}{\mathrm{d}t} = -\sum_j m_j \left(\frac{\sigma_i^{\alpha\beta}}{\rho_i^2} + \frac{\sigma_j^{\alpha\beta}}{\rho_j^2} + \Pi_{ij}\right)W_{ij,\beta}, \tag{19}$$

$$\frac{\mathrm{d}e_i}{\mathrm{d}t} = \sum_j m_j (v_i^\alpha - v_j^\alpha)\left(\frac{\sigma_i^{\alpha\beta}}{\rho_i^2} + \frac{1}{2}\Pi_{ij}\right)W_{ij,\beta} \tag{20}$$

and

$$\frac{\mathrm{d}S_i^{\alpha\beta}}{\mathrm{d}t} = \frac{\mu}{2}\sum_j \frac{m_j}{\rho_j}\left[(v_i^\alpha - v_j^\alpha)W_{ij,\beta} + (v_i^\beta - v_j^\beta)W_{ij,\alpha} - \frac{1}{3}(v_i^\gamma - v_j^\gamma)W_{ij,\gamma}\right] + \dot{S}_i^{\alpha\gamma}\dot{R}_i^{\beta\gamma} + \dot{S}_i^{\gamma\beta}\dot{R}_i^{\alpha\gamma}. \tag{21}$$

In eqs (18)–(21), $W_{ij} = W(\boldsymbol{x}_i - \boldsymbol{x}_j, h_{ij})$ is the kernel function with smoothing length $h_{ij} = (h_i + h_j)/2$ where h_i denotes the smoothing length associated with the ith particle. In this article, the cubic spline kernel function, given in the following equation, is used.

$$W(q, h) = \alpha_D \begin{cases} 1 - \frac{3}{2}q^2 + \frac{3}{4}q^3 & 0 \le q \le 1, \\ \frac{1}{4}(2-q)^3 & 1 \le q \le 2, \\ 0 & q \ge 2, \end{cases} \tag{22}$$

where $\alpha_D = 10/7\pi h^2$ in $2D$.

The artificial viscosity term Π_{ij} in eqs (19) and (20) is given by[3],

$$\Pi_{ij} = \frac{-\alpha_1 c_{ij}\mu_{ij} + \alpha_2\mu_{ij}^2}{\rho_{ij}}$$

$$\text{if } r_{ij} \cdot v_{ij} < 0 \text{ otherwise } \Pi_{ij} = 0 \tag{23}$$

where

$$\mu_{ij} = \frac{h_{ij}\boldsymbol{r}_{ij} \cdot \boldsymbol{v}_{ij}}{r_{ij}^2 + \varepsilon h_{ij}^2} \tag{24}$$

$c_{ij} = (c_i + c_j)/2$, $r_{ij} = x_i - x_j$, $v_{ij} = v_i - v_j$ and $r_{ij} = \|r_{ij}\|$,

where (α_1, α_2) are the artificial viscosity parameters. In eq. (30), ε is introduced to prevent a singularity when $r_{ij} = 0$ and is generally taken as 0.01 (ref. 3).

Acceleration correction algorithm

The method

Before proceeding to outline the acceleration correction algorithm[9], two observations relating to the use of this algorithm are given here.

(i) The amount of dissipation an artificial viscosity generates, whilst removing the unphysical oscillation behind the shock front, depends mainly on the choice of α_1 and α_2 has itself an insignificant effect on the overall dissipation[10,11].

(ii) Some commonly (though heuristically ascribed) used values of[4,6,7,12] (α_1, α_2) are (0.5, 0.5), ($0.2 \le \alpha \le 0.5$, $0.5 \le \beta \le 4.0$), (1.0, 2.0), (1.0, 1.0), etc. Some authors have also used[5,7,12] (2.5, 2.5). However nothing is mentioned about the reason for choosing this large value of α_1. Based on some numerical experiment (a similar experiment is also performed herein, see the fourth section) it is shown in Shaw and Reid[9] that an SPH computation in solid mechanics can generally be stabilized with $\alpha_1 \le 1$.

An intrinsic feature of the correction algorithm is that (α_1, α_2) is set *ab initio* equal to (1, 1) in all of the impact examples of the correction algorithm calculations performed by the authors to date. It should be noted that, to provide a direct comparison with the SPH solution of

Libersky and Petschek[4], values of (0.5, 0.5) were adopted in the uncorrected version of SPH (based on equations 18–21) to compare with the corrected version in figure 6 *b*. It should be noted that, in general, (α_1, α_2) are not arbitrarily, user-defined parameters in the version of the correction algorithm illustrated in this article.

Thus, the first step in the heuristic algorithm is to set the parameters (α_1, α_2) in eq. (24) to (1, 1). Consequently the form of the artificial viscosity becomes

$$\Pi_{ij}^{(1,1)} = \frac{-c_{ij}\mu_{ij} + \mu_{ij}^2}{\rho_{ij}}$$

$$\text{if } r_{ij}\cdot v_{ij} < 0 \text{ otherwise } \Pi_{ij}^{(1,1)} = 0. \tag{25}$$

Using the artificial viscosity given by eq. (24), the momentum eq. (19) may be rewritten as

$$\frac{\mathrm{d}v_i^\alpha}{\mathrm{d}t} = -\sum_j m_j \left(\frac{\sigma_i^{\alpha\beta}}{\rho_i^2} + \frac{\sigma_j^{\alpha\beta}}{\rho_j^2} \right) W_{ij,\beta} - \sum_j m_j \Pi_{ij}^{(1,1)} W_{ij,\beta}. \tag{26}$$

Following the observations (i) and (ii), it is reasonable to consider that eq. (25) is an overestimation of the artificial viscosity and may introduce unwanted dissipation into the system. This unwanted dissipation is removed by including a correction term into eq. (26) as

$$\frac{\mathrm{d}v_i^\alpha}{\mathrm{d}t} = -\sum_j m_j \left(\frac{\sigma_i^{\alpha\beta}}{\rho_i^2} + \frac{\sigma_j^{\alpha\beta}}{\rho_j^2} \right) W_{ij,\beta}$$

$$-\sum_j m_j \Pi_{ij}^{(1,1)} W_{ij,\beta} - d\overline{a}_i^\alpha \tag{27}$$

where $d\,\overline{a}_i^\alpha$ is taken as

$$d\overline{a}_i^\alpha = \frac{1}{2}\sum_j (da_i^\alpha + da_j^\alpha)\overline{W}_{ij}\ , \tag{28}$$

with $\overline{W}_{ij} = W(\boldsymbol{x}_i - \boldsymbol{x}_j, \overline{h})$ and $\mathrm{d}a_i^\alpha = -\sum_{j=1}^{N} m_j \Pi_{ij}^{(1,1)} W_{ij,\beta}$.

The basis for choosing the smoothing lengths h_i and $\overline{h}$ are discussed in in the next subsection. Now, using eqs (27) and (28), the corrected momentum equation may be written as

$$\frac{\mathrm{d}v_i^\alpha}{\mathrm{d}t} = -\sum_j m_j \left(\frac{\sigma_i^{\alpha\beta}}{\rho_i^2} + \frac{\sigma_j^{\alpha\beta}}{\rho_j^2} \right) W_{ij,\beta} \underbrace{-\sum_i m_j \Pi_{ij}^{(1,1)} W_{ij,\beta}}_{\text{Dissipation term}}$$

$$\underbrace{+\frac{1}{2}\sum_j \left(\sum_k m_k (\Pi_{ik}^{(1,1)} W_{ik,\beta} + \Pi_{jk}^{(1,1)} W_{jk,\beta}) \right) \overline{W}_{ij}}_{\text{Correction term}}\ . \tag{29}$$

The energy eq. (22) is modified correspondingly as

$$\frac{\mathrm{d}e_i}{\mathrm{d}t} = \sum_j m_j (v_i^\alpha - v_j^\alpha) \left(\frac{\sigma_i^{\alpha\beta}}{\rho_i^2} \right) W_{ij,\beta}$$

$$\underbrace{+\frac{1}{2}\sum_j m_j (v_i^\alpha - v_j^\alpha) \Pi_{ij}^{(1,1)} W_{ij,\beta}}_{\text{Dissipation term}}$$

$$\underbrace{-\frac{1}{2}\sum_j (v_i^\alpha - v_j^\alpha) \left(\sum_k m_k \Pi_{jk}^{(1,1)} W_{jk,\beta} \overline{W}_{ik} \right)}_{\text{Correction term}}. \tag{30}$$

The main difference between the standard SPH and SPH with the acceleration correction algorithm lies in the formulation of the momentum and energy equations (see eqs (19), (20), (29), (30)). By doing this, some of the problematic dissipation of energy is removed in a manner that does not disturb the stability of the numerical solution, since the basic effect of the artificial viscosity is retained. However the 'loss' of energy is reduced to the benefit of the physicality of the solution.

Calculation of smoothing lengths (h_i and $\overline{h}$)

The accuracy of SPH computations greatly depends on the choice of the smoothing length. Some SPH computations assume that h_j is same for all particles, while others prefer to use a spatially and temporally variable h_j[13,14]. Both approaches have their own merits and demerits. It is desirable to use a variable h_j (smaller for high particle density regions and larger for low particle density regions for any instant of time) in order to capture the local behaviour and maintain the same level of accuracy everywhere in the computational domain. However, the inclusion of the additional term which accounts for the variablitiy of the smoothing length, makes the computation more numerically intensive[14].

As far as the problems related to solid mechanics are concerned, one major advantage is, the normally strong cohesion between two particles. Therefore even in very large deformation processes, one particle cannot move too far from its neighbouring particle unless there is a fracture or fragmentation of the material. Therefore, if the initial particle distribution is quasi-uniform, it is reasonable to take a constant $h_i = h$ for all particles. We observed that approximately 25–30 neighbours per particle yields reasonably good results (in the context of TREESPH Hernquist and Katz suggested 30–40 neighbours per particle). The smoothing length $\overline{h}$ for the correction term is chosen such that each particle interacts only with its nearest neighbours as shown in Figure 1.

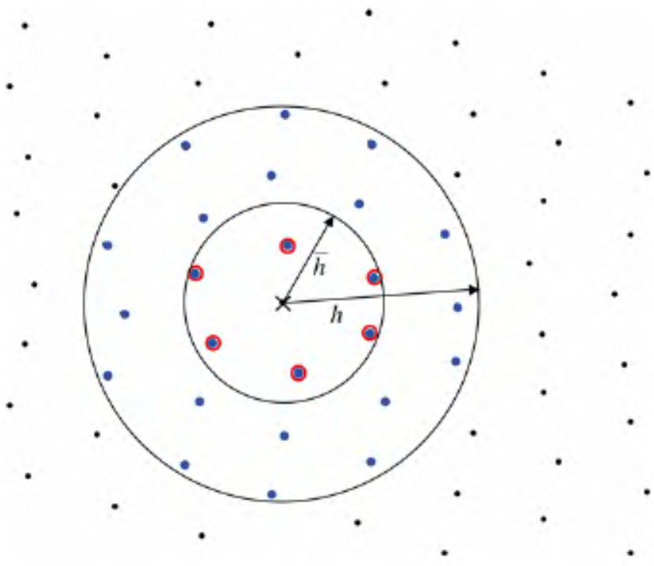

Figure 1. Smoothing lengths (h_i and $\bar{h}$).

Numerical examples

Example 1: Taylor impact problem

A 2D plane-strain model[4] of an iron rod travelling at 200 m/s which impacts a rigid surface as shown in Figure 2 is considered. In Libersky and Petschek[4], the rod was discretized by $21 \times 67 = 1407$ particles and the smoothing length h was taken as 0.0076 m. The rigid wall was modelled by ghost particles[15], placed outside the wall. The artificial viscosity parameters were taken as (0.5, 0.5). The same problem is re-visited here. In order to permit a valid comparison, all relevant data (geometric, material and numerical) were taken as given in Libersky and Petschek[4].

In order to see the effect of artificial viscosity *per se*, first an attempt is made to solve the problem without any artificial viscosity ($\alpha_1 = 0$, $\alpha_2 = 0$). The deformed shape of the iron rod at 50 μs is shown in Figure 3. It seems that particles crumble at the impact end of the rod. This is not consistent with experimental observations or with the results given in Libersky and Petschek[4]. This numerical fracture may be ascribed to the instability due to the presence of high frequency oscillation near the shock front caused by the initial discontinuous velocity profile between the rod and the rigid wall. By introducing some dissipation in the form of artificial viscosity one may stabilize the numerical computation. However, the strength of artificial viscosity (or in other words the value of (α_1, α_2)) required to run the problem without experiencing any numerical fragmentation and instability is not known *a priori*. Most of the SPH computations are performed with some heuristically-taken (α_1, α_2) irrespective of the particle distribution, choice of kernel function or the smoothing length. Therefore the accuracy of the prediction through SPH computation with an arbitrarily chosen (α_1, α_2) is generally questionable. In order to show how the choice of the artificial viscosity parameters significantly affect the accuracy of the solution, a numerical experiment using the basic SPH equations (eqs (18)–(21)) was performed with different values of (α_1, α_2). Figure 4 shows the deformed shape of the rod at 50 μs obtained with different (α_1, α_2). It can be seen that the impact (proximal) end of the rod experiences less bulging as (α_1, α_2) increases. This may be ascribed to the artificial viscosity which acts as an energy sink and produces spurious entropy into the system. This is also evident in the computed kinetic energy shown in Figure 5. These observa-

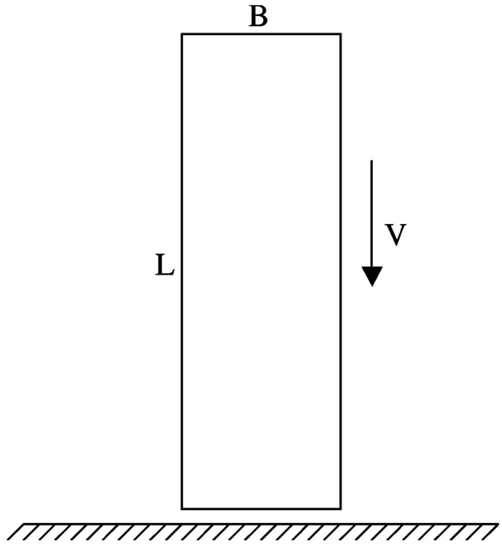

Figure 2. Iron rod impact impacting a rigid surface normally (example 1). Parameters are given in Table 1.

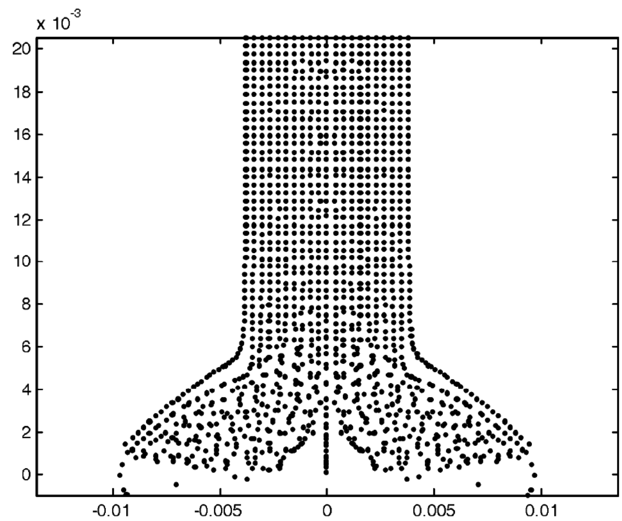

Figure 3. Deformation of the iron rod at 50 μs as computed by SPH without any artificial viscosity, i.e. (α_1, α_2) = (0, 0) in eqs (19) and (20).

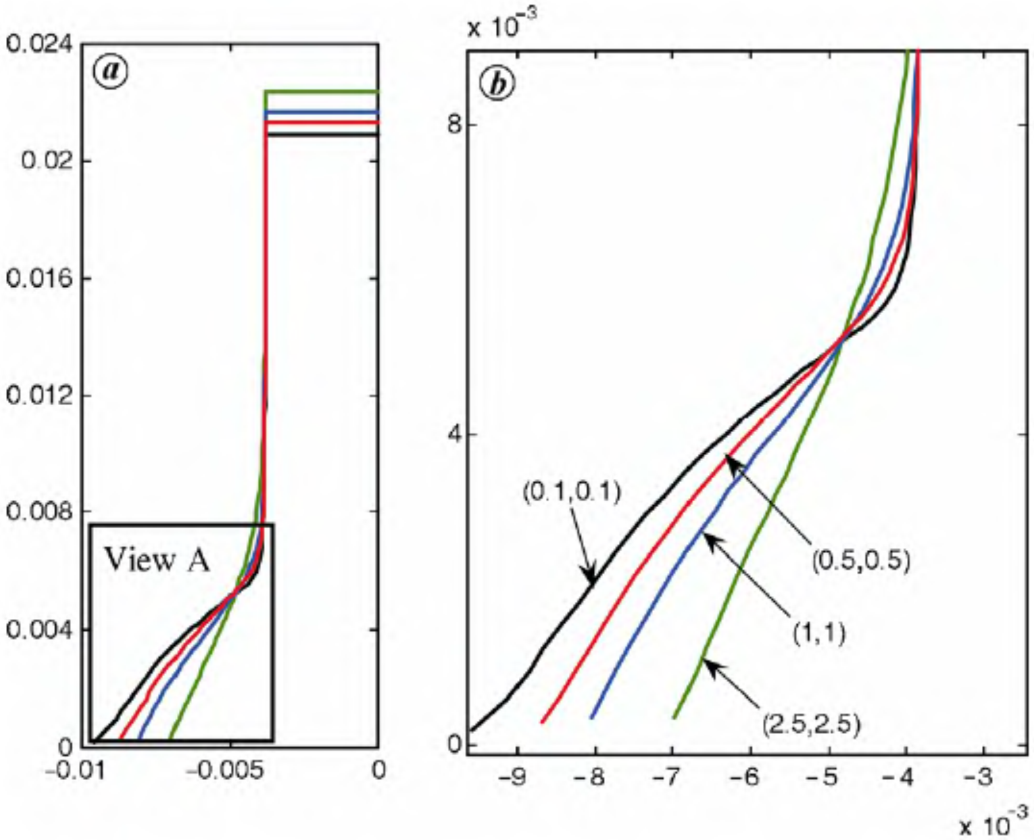

Figure 4. ***a***, Deformation of the iron rod at 50 μs as computed by the uncorrected SPH with different values of (α_1, α_2) in eqs (18) and (19); ***b***, view A.

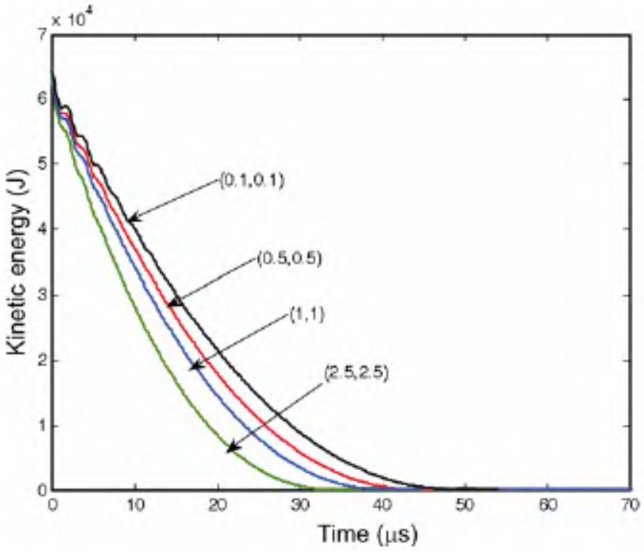

Figure 5. Computed kinetic energy for the uncorrected SPH (eqs (18)–(21) with different values of (α_1, α_2).

tions explain the discrepancy between the results obtained via SPH and the EPIC-2 code as reported in Randles and Libersky[15].

Now, running the program with the acceleration correction algorithm, the deformed shapes of the rod at 50 μs obtained via SPH and the EPIC-2 code are compared in Figure 6. It can be seen from this figure that the standard SPH with ($\alpha_1 = 0.5$, $\alpha_2 = 0.5$) result indeed shows less bulging than that predicted by the EPIC-2 code as previously observed by Libersky and Petschek[4]. However, the computed deformation using SPH with the acceleration algorithm is in very close agreement with the EPIC-2 code result.

Example 2: Parkes cantilever beam

In order to understand the role of elasticity in structures undergoing impact loading, Reid and Gui[16] examined the transient behaviour of an elastic-perfectly plastic cantilever beam carrying a tip mass which is subjected to a impulsive loading as shown in Figure 7 (often referred to as the Parkes cantilever problem[17]). Using an FEM model in ABAQUS, it was shown that during the initial stage of the deformation process a plastic region (hinge) is formed near the tip and starts propagating from the tip towards the root. However due to the reflected precursor elastic wave the progress of the plastic hinge is arrested at approximately the centre, giving the beam a characteristic local 'kink' there and delaying the root rotation phase of the beam. This phenomenon was the key contribution of Reid and Gui[16].

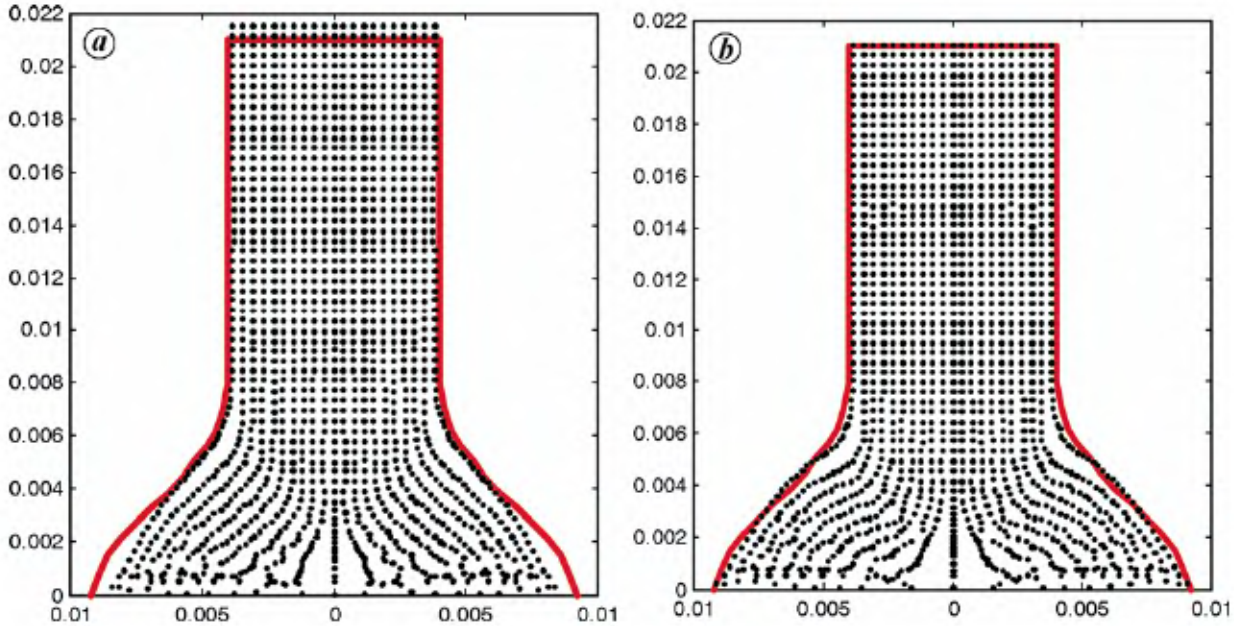

Figure 6. Deformation of the iron rod at 50 μs as computed by (***a***) uncorrected SPH ($\alpha_1 = 0.5$, $\alpha_2 = 0.5$) and (***b***) SPH using the acceleration correction algorithm as described in section 'Acceleration correction algorithm'. Results obtained via EPIC-2 code (Libersky and Petschek[4]) are shown by bold line.

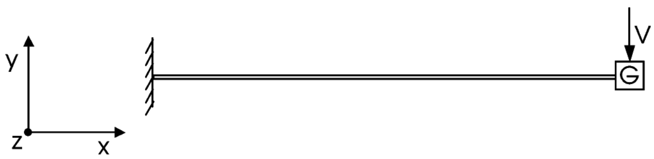

Figure 7. Cantilever beam with tip mass.

For a given geometric and material properties, the initial condition of the beam is defined by a non-dimensional quantity called energy ratio, given by

$$R = \frac{\text{Initial kinetic energy}}{\text{Maximum elastic strain energy}} = \frac{GV_0^2 EI}{M_0^2 L}, \tag{31}$$

where G and V_0 are respectively the mass and initial velocity of tip mass, L the length of the beam, M_0 the fully plastic moment of the beam, E the Young's modulus of the material and I the moment of inertia of beam cross-section. It was shown in Symonds and Fleming[18], that the transient behaviour of the beam significantly depends on R. The final tip deflection and the amount of plastic work done during the beam deformation increase with increase in R.

The presence of a source of dissipation in a numerical simulation (like artificial viscosity in SPH) results in the reduction of effective kinetic energy and thus the effective R used in the simulation. Hence this problem can be used as a useful example in order to study the effect of artificial viscosity and the efficacy of the acceleration correction algorithm.

Table 1. Parameters used in the Taylor bullet impact test simulations

Parameter	Values
E (MPa)	2.08×10^5
μ (MPa)	80×10^3
σ_y (MPa)	600
L (m)	0.0254
B (m)	0.0076
V (m/s)	200
C (cm/μs) (in eq. (10))	0.36
S (in eq. (11))	1.80
Γ (in eq. (7))	1.80

In this section, the Parkes cantilever problem is re-revisited via the SPH method. Results obtained with and without the acceleration correction algorithm are compared with those given in Reid and Gui[16]. The geometry and the material properties of the beam as considered in table 1, example 2 in Reid and Gui[16] are given in Table 2. Values for parameters C, S and Γ are taken same as given in the previous example (see Table 1) are taken here.

The beam is discretized by 201×5 particles as shown in Figure 8*a*. A uniform smoothing length $h = 1.3\Delta x$ (corresponds to 30 particles on average within the support of the B-spline kernel function given by eq. (22)) is taken. Since a 2D plane strain model of the beam is considered, the width (dimension along z-axis) of the beam is assumed to be one. Consequently, the total mass of the beam is taken as ρLd instead of the original mass ρLdb. Therefore in order to keep the mass ratio (β) same, we scale the tip mass as

$$\bar{G} = \frac{G}{b}. \tag{32}$$

Figure 8. ***a***, Discretization of the cantilever beam by 201 × 5 particles; ***b***, Tip mass is distributed over a small region near the tip; ***c***, Tip mass is equally distributed over 5 × 5 particles (shown by red circle) at the tip.

Table 2. Material and geometrical properties of the cantilever beam shown in Figure 2

Parameters	Value
E (N/mm^2)	2.069×10^5
σ_0 (N/mm^2)	344
M_0 (Nm)	24.8
ρ (kg/m^3)	7493
L (mm)	304.8
b (mm)	6.6
h (mm)	6.6
G (kg)	0.0023
$\beta = \rho Lbd/2G$	21.96
V_0 (m/s)	481.6
K_0 (J)	137.4

Using a similar approach to that adopted by Reid and Gui[16], the tip mass is modelled as an extra mass distributed over 5 × 5 = 25 particles near the tip of the cantilever beam as shown in Figure 8 *b*. Masses and initial densities of these particles are modified as

$$\bar{m}_i = m_i + \frac{\bar{G}}{25},$$

$$\bar{\rho}_i = \frac{\bar{m}_i}{\Delta V_i^0},$$

where ΔV_i^0 is the initial nodal volume obtained through a Voronoi tessellation.

The initial velocity of the particles over which the tip mass is distributed is calculated based on the conservation of momentum as

$$\bar{V}_0 = \frac{\bar{G}}{\bar{M}} V_0, \tag{33}$$

where $\bar{M}$ is the total mass of the particles over which the tip mass is distributed. For the given discretization (see Figure 8), $\bar{V}_0 = 241.1$ m/s and the initial kinetic energy K_0 of the system is 135.17 J.

It was observed through a numerical experiment that an SPH computation becomes unstable for $\alpha_1 < 0.1$, irrespective of value of α_2. Therefore (0.1, 0.1) is considered as the optimum value for (α_1, α_2) for the problem (with given particle distribution, smoothing length and kernel) under consideration.

Extreme elastic vibration positions after all the plastic deformation has occurred obtained via the SPH with $\alpha_1 = 0.1$ and SPH with acceleration correction algorithm are compared with the FEM solution[16] in Figure 9 *a* and *b*. It can readily be seen that although the SPH with the 'optimum' choice of artificial viscosity parameter does not experience any instability (or numerical fragmentation), the extreme elastic vibration positions are far less accurate than those obtained via FEM. Whereas the deformed shapes obtained via the SPH with the acceleration correction algorithm are in very good agreement with the FEM results.

Note however that deformation of the impact end is not as curled as in the FEM solution. This may be explained by the effect of plastic shearing close to the projectile. This was not taken into consideration in FEM analysis[16] which used elements that could only sustain elastic shear. This new SPH approach provides the opportunity to investigate this and other important features in such problems. A more in-depth study of this additional information will be the subject of a future paper.

The variation with time of the computed total kinetic energy of the beam obtained via SPH with $\alpha_1 = 0.1$ and SPH with acceleration correction algorithm are compared in Figure 10 and the superiority of the acceleration correction algorithm can easily be observed.

Closure

Artificial viscosity in SPH computations, is a numerical necessity which requires some user-defined parameters. Free choice of these parameters may lead to spurious

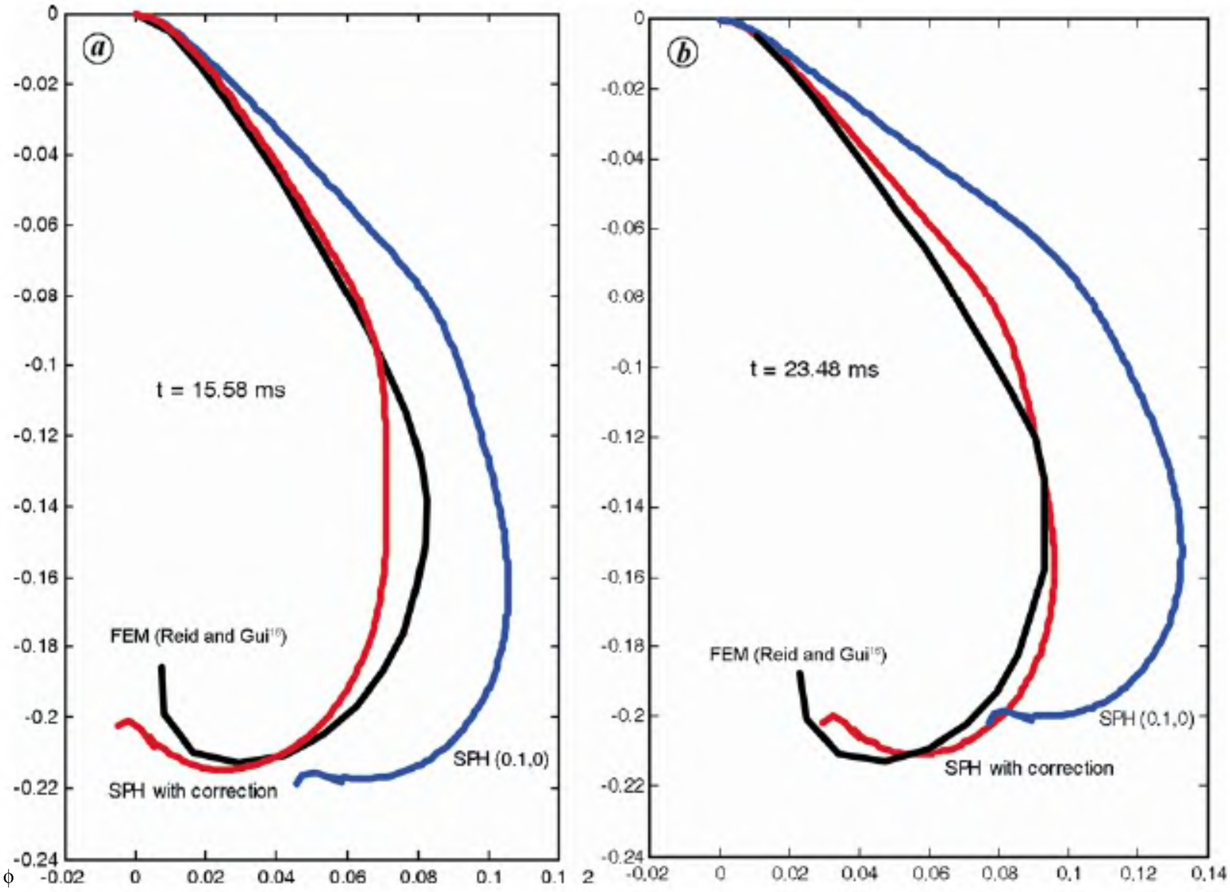

Figure 9. Extreme elastic vibration positions of neutral axis after all plastic deformation complete (***a***) maximum at t = 15.80 ms and (***b***) minimum at t = 23.50.

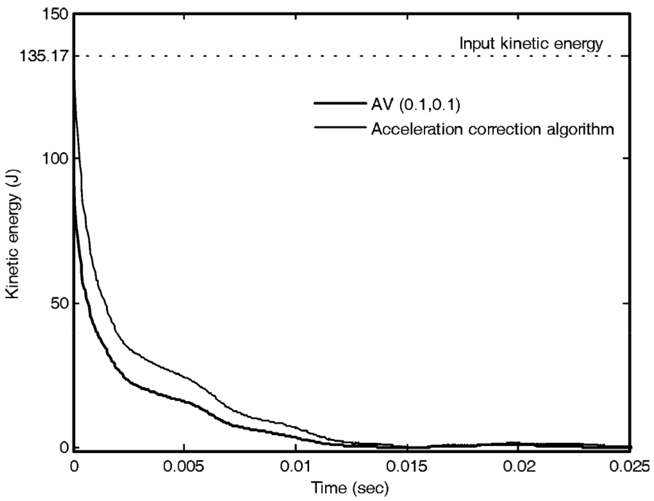

Figure 10. Computed kinetic energy of beam.

entropy production into the system and make it over-dissipative. This is of particular concern in impact mechanics problems where the transient behaviour of the structure in many cases depends significantly on the transfer of momentum and kinetic energy from a projectile to the structure. In order to circumvent the above difficulty, an acceleration correction algorithm has been proposed in Shaw and Reid[9].

The essence of the method is to calculate the change in the acceleration due to the artificial viscosity term and then correct the computed acceleration by subtracting a convex approximation of the 'changed' acceleration. The governing equations, in particular energy equation, are accordingly modified. It is shown in Shaw and Reid (ref. 9) that the acceleration correction algorithm does not need any user specified parameters and yet stabilizes the numerical computation without adding substantially unwanted dissipation into the system.

Some numerical aspects of the acceleration correction algorithm are discussed here and the method is further explored in the context of two classical impact problems, the Taylor bullet impact problem and the dynamic, elastic-plastic deformation of a cantilever beam subjected to tip impact – the 'Parkes problem'. Results obtained via the SPH with the acceleration correction algorithm are compared with the uncorrected SPH solution given in Libersky and Petschek[4] for the Taylor bullet impact problem and with the FEM solution given by Reid and Gui[16] for the Parkes problem. More details of the latter and related problems will be given in a forthcoming paper.

The superior performance of the acceleration correction algorithm which does not require a set of numerical experiments vis-à-vis the SPH procedures with the 'optimum' artificial viscosity has been discussed and the efficacy of the new method demonstrated for typical impact problems.

1. Gingold, R. A. and Monaghan, J. J., Smoothed particle hydrodynamics: theory and application to non-spherical stars. *MNRAS*, 1977, **181**, 275–389.
2. Lucy, L., A numerical approach to testing the fission hypothesis. *Astron. J.*, 1977, **82**, 1013–1024.
3. Monaghan, J. J., Smoothed particle hydrodynamics. *Annu. Rev. Astron. Astrophys.*, 1992, **30**, 543–574.
4. Libersky, L. D. and Petschek, A. G., Smoothed particle hydrodynamics with strength of materials. In *Proceedings of the Next Free Lagrange Conference* (eds Trease, H., Fritts, J. and Crowley, W.), Springer-Verlag, NY, 1991, vol. 395, pp. 248–257.
5. Libersky, L. D., Petschek, A. G., Carney, T. C., Hipp, J. R. and Allahdadi, F. A., High strain Lagrangian hydrodynamics a three-dimensional SPH code for dynamic material response. *J. Comput. Phys.*, 1993, **109**, 67–75.
6. Johnson, G. R., Stryk, A. R. and Beissel, S. R., SPH for high velocity impact computations. *Comput. Methods Appl. Mech. Eng.*, 1996, **139**, 347–373.
7. Mehra, V. and Chaturvedi, S., High velocity impact of metal sphere on thin metallic plates: a comparative smooth particle hydrodynamics study. *J. Comput. Phys.*, 2006, **112**, 318–337.
8. Benz, W. and Asphaug, E., Simulation of brittle solids using smooth particle hydrodynamics. *Comp. Phys. Commun.*, 1995, **87**, 253–265.
9. Shaw, A. and Reid, S. R., Heuristic acceleration correction algorithm for use in SPH computations in impact mechanics. *Comput. Methods Appl. Mech. Eng.*, 2009; doi: 10.1016/j.cma.2009.09.006.
10. Caramana, E. J., Shashkov, M. J. and Whalen, P. P., Formulations of artificial viscosity for multi-dimensional shock wave computations. *J. Comput. Phys.*, 1998, **144**, 70–97.
11. Johnson, G. R., Artificial viscosity effects for SPH impact computations. *Int. J. Impact Eng.*, 1996, **18**, 477–488.
12. Seo, S., Min, O. and Lee, J., Application of an improved contact algorithm for penetration analysis in SPH. *Int. J. Impact Eng.*, 2008, **32**, 578–588.
13. Hernquist, L. and Katz, N., TREESPH: a unification of SPH with the hierarchical tree method. *Astrophys. J. Series*, 1989, **70**, 419–446.
14. Nelson, R. P. and Papaloizou, J. C. B., Variable smoothing length and energy conservation in smoothed particle hydrodynamics. *Mon. Not. Astron. Soc.*, 1994, **270**, 1–20.
15. Randles, P. W. and Libersky, L. D., Smoothed particle hydrodynamics: some recent improvements and applications. *Comput. Methods Appl. Mech. Eng.*, 1996, **139**, 375–408.
16. Reid, S. R. and Gui, X. G., On the elastic-plastic deformation of cantilever beams subjected to tip impact. *Int. J. Impact Eng.*, 1987, **6**, 109–127.
17. Parkes, E. W., The permanent deformation of a cantilever struck transversely at its tip. *Proc. R. Soc. A*, 1955, **288**, 462.
18. Symonds, P. S. and Fleming Jr, W. T., Parkes revisited: on rigid-plastic and elastic-plastic dynamic structural analysis. *Int. J. Impact Eng.*, 1984, **2**, 1–36.